

Iron point defect reduction in multicrystalline silicon solar cells

Matthew D. Pickett^{1,a)} and Tonio Buonassisi^{2,b)}

¹*Department of Materials Science and Engineering, University of California, Berkeley, California 94720, USA*

²*Department of Mechanical Engineering, Massachusetts Institute of Technology, Cambridge, Massachusetts 02139, USA*

(Received 8 January 2008; accepted 26 February 2008; published online 25 March 2008)

In this work, we propose and demonstrate an annealing procedure designed to improve the performance of iron-contaminated silicon solar cells. Specifically, we put forward the idea that cells contaminated with iron should be annealed at appropriate times and temperatures to allow for the transformation from supersaturated point defects to distributed iron silicide precipitates. We examine the optimal transformation rate for string ribbon multicrystalline silicon and demonstrate that a 30 min annealing can improve the efficiency of cells manufactured from low-purity feedstock. © 2008 American Institute of Physics. [DOI: 10.1063/1.2898204]

Transition metal contamination in silicon has always been a significant concern for silicon device manufacturers due to the strong device degradation it can cause. Iron contamination is especially problematic because the element has a high solubility and diffusivity at device processing temperatures; it can serve as an active deep donor with a significant capture cross section, and it is ubiquitous even in clean room environments.¹ Thus, industrial necessity has motivated decades of research into the materials science of iron in silicon (see the extensive reviews by Istratov *et al.*^{1,2}).

In silicon photovoltaics (PV), manufacturers cannot utilize many of the developments made by integrated circuit makers because of cost limitations. Therefore, solar cell manufacturers are forced to make a compromise, based on cost and performance, between different feedstock purities and crystal growth techniques. As a result of this compromise, as-grown multicrystalline silicon (mc-Si) PV materials typically contain a total of 10^{14} – 10^{15} Fe atoms cm^{-3} .^{3,4} Even in the slowly cooled directional solidification growth technique, a significant fraction (Macdonald *et al.* measured $\sim 1\%$ or 10^{12} cm^{-3} , Ref. 4) of these atoms does not precipitate during growth and remain supersaturated in the highly detrimental interstitial point defect form. Additionally, high-temperature processing can cause dissolution of some of the precipitated iron, therefore limiting the effectiveness of gettering and passivation.^{5,6} Because of this situation, PV manufacturers must continue to develop processes that are tolerant to high levels of Fe contamination, especially with the move toward cheaper feedstocks.

In this work, we propose and experiment on an isothermal annealing process, based on iron precipitation kinetics, intended to reduce iron point defect concentrations in mc-Si solar cells. The annealing is designed to result in the nucleation and/or growth of iron silicide precipitates at the expense of the more detrimental Fe point defects, an idea outlined previously by Plekhanov *et al.*⁵ and Buonassisi *et al.*⁷ To provide the optimal conditions for Fe precipitation, the temperature must be sufficiently low to result in a high degree of supersaturation and sufficiently high to allow for dif-

fusion to and aggregation at nucleation sites. The optimal temperature is quantitatively dictated by total Fe content, Fe diffusivity, and the spatial distribution of heterogeneous nucleation sites. Henley *et al.*⁸ and Haarahiltunen *et al.*⁹ have investigated Fe silicide nucleation kinetics in this way in floating zone and Czochralski materials, respectively, and both indicate an optimal temperature of around 500 °C. Here, we expand and apply this work to a mc-Si solar cell process.

In order to test the impact of isothermal annealing on iron precipitate growth and the resulting impact on device characteristics, we conducted two experiments. In the first experiment, we characterized the temperature dependence of Fe precipitation in mc-Si by testing Fe rich samples. The samples we used were *p*-type wafers of mc-Si grown from Fe rich feedstock with the string ribbon method at Evergreen Solar. The “Fe rich” feedstock contained roughly 100 ppb (parts per billion) of iron. Before dividing the wafers into sample sets, we randomized them to account for any time-dependent variation that occurred in the melt (due to segregation or other effects). Then, we annealed the wafers at a constant temperature for 30 min in a tube furnace (in a 96% Ar and 4% H₂ ambient) and measured the remaining iron-boron (Fe_i–B_s) pair concentrations. For the Fe_i–B_s concentration measurements, we used a Semilab microwave photoconductivity decay mapping tool equipped with a flash lamp for pair dissociation.

In the second experiment we tested the application of a precipitate forming annealing on a commercial solar cell production process. As summarized in Table I, we processed a test matrix of two different batches of string ribbon wafers grown using two different processes. The two groups of wafers we used were samples of the iron rich batch (batch 1) described in the previous paragraph and a batch of randomized samples of wafers grown from a high-purity feedstock (batch 2). The “high-purity” feedstock contained roughly 1 ppb of iron. The two different cell processes we applied were a factory inspired reference process (process A) and the same process with the addition of a 30 min annealing at 500 °C after the phosphorous emitter diffusion, but before the glass etch (process B). After fabricating the four groups, we measured the illuminated *IV* curves and then calculated

^{a)}Present address: Hewlett-Packard Laboratories, Palo Alto, CA. Electronic mail: matthew.pickett@hp.com.

^{b)}Formerly at Evergreen Solar, Inc., Marlborough, Massachusetts.

TABLE I. The constituents of the 2×2 test matrix that we used to test the impact of a 30 min, 500 °C annealing on iron contaminated mc-Si solar cells following phosphorous diffusion, but before glass etch, with results.

Wafer batches	Cell process	
	Process A: Factory-inspired reference process	Process B: Addition of isothermal annealing after P diffusion
Batch 1: Wafers grown with iron rich feedstock (~ 100 ppb Fe)	Control	Cell efficiency=2.2% (relative) higher than process A (control) Short circuit current=1.2% (relative) higher than process A
Batch 2: Wafers grown with high-purity feedstock (~ 1 ppb Fe)	Control	Efficiency and short circuit current not statistically different from process A (control)

the cell efficiency and short circuit current values from the curves.

The results of the first experiment are included in Fig. 1. Not surprisingly, there is a significant spread in the data due to the material inhomogeneities, but the statistical features are nevertheless clear. The isothermal annealing above 500 °C changed the iron-boron pair concentration widely for different samples but the average change is close to zero. In contrast, the annealing below 500 °C all resulted in a net pair decrease of around 10%–20%. Because of our large sample-to-sample variations and limited sample size, we are hesitant to assign a precise value for the optimal annealing temperature. However, from these results, it seems reasonable to state that the range of 400–500 °C is a good starting point for optimization which is consistent with the results in Refs. 8 and 9.

The results of the second experiment showed that the application of a 30 min precipitation annealing can significantly improve the device characteristics of wafers grown from iron rich feedstock. In Fig. 2, we compare the control and experimental processes (A and B) for batch 1, the iron rich batch. The addition of the annealing step in process B resulted in a median 1.2% (relative) increase in the short circuit current and a median 2.2% (relative) increase in the efficiency compared to the median values of the reference process (process A). As with the results of the first experiment, the large spread in the data is due to the material and process variability which we attempted to distribute uniformly across sample sets by randomization. We do not include a figure containing a comparison of the results for batch 2 (grown with high-purity feedstock), because it did not exhibit a statistical difference between processes A and

B. Because of this fact, we conclude that the device characteristics of batch 2 are not limited by iron defects.

The implications of precipitate forming annealing on cell fabrication are multiple. First, as industrial solar cell architectures and efficiencies improve, they will become more sensitive to the bulk minority carrier lifetime, and as such, residual $\text{Fe}_i\text{-B}_s$ concentrations. The annealing guidelines demonstrated herein thus have the potential to further improve the performance of high-efficiency solar cell devices, possibly even those made of high-purity feedstocks.

Second, the effect of hydrogen passivation must be re-evaluated, in the context of redistributing point defects. While other passivation processes are likely to occur, part of the beneficial impact of H passivation during SiN_x firing (typically performed between 400 and 500 °C) on mc-Si material may be partially due to the redistribution of Fe point defects. This effect is expected to be strongest in material

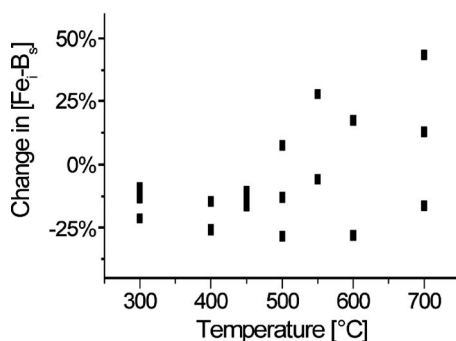


FIG. 1. Percentage change in the iron boron point defect concentration of Fe rich mc-Si wafers vs 30 min isothermal annealing temperature.

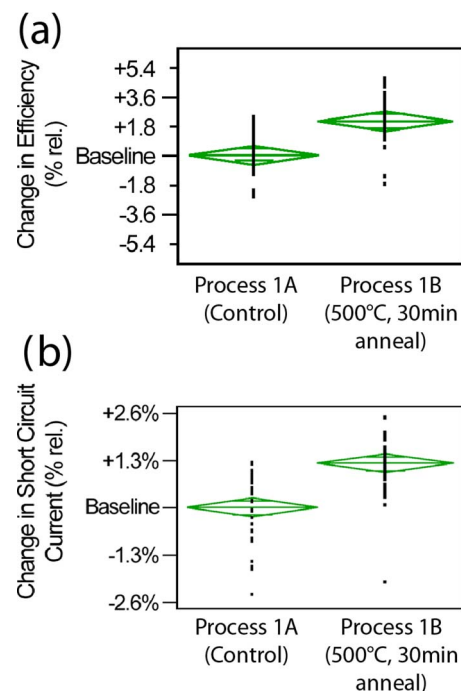


FIG. 2. (Color online) Percentage change, relative to the base line, of the (a) cell efficiency and (b) short circuit current for the sample sets 1A and 1B. Set 1A consisted of wafers from the Fe rich batch fabricated with the reference process while set 1B was grown and processed identically to 1A with the addition of a 30 min 500 °C annealing after phosphorous diffusion.

with high as-grown Fe point defect concentrations and sub-optimal P-diffusion annealing. In a sense, SiN_x firing, by virtue of its temperature alone, may be able to compensate for suboptimal processing and material quality.

Third, the influence of the last high-temperature step of solar cell processing, i.e., contact metallization firing, must be carefully evaluated in terms of dissolving and redistributing precipitated Fe atoms. Other researchers have shown that precipitate redissolution can occur within tens of seconds.^{5,6,10} For this reason, short firing times and low temperatures are preferred.

Fourth, long annealing will eventually drive the iron-boron pair concentration down to the equilibrium solubility level at the annealing temperature. Depending on the feedstock and manufacturing cost model, it may make sense to anneal at somewhere around 400–500 °C for several hours to obtain even better device efficiency. This is a parameter space that, to our knowledge, remains largely unexplored in the context of iron silicide nucleation and growth.

Last, this approach should be applied to all impurity species in mc-Si that are more recombination active as point defects than they are as precipitates. This was proposed¹¹ in a less general way with respect to chromium defects but has since not been widely discussed. Note that the optimum annealing temperature is a function not only of element-dependent properties, such as diffusivity and solubility, but also the concentration of a given metallic species and the density of heterogeneous nucleation sites. Nevertheless, one could envision an annealing consisting of multiple plateaus

to encourage precipitation of several transition metal species.

We would like to acknowledge Robert Sweeney for the processing assistance. M.D.P. would like to thank the Intel Foundation for support from a Robert Noyce Fellowship during this research project. Doug Spreng is acknowledged for his support of this research.

¹A. A. Istratov, H. Hieslmair, and E. R. Weber, *Appl. Phys. A: Mater. Sci. Process.* **70**, 489 (2000).

²A. A. Istratov, H. Hieslmair, and E. R. Weber, *Appl. Phys. A: Mater. Sci. Process.* **69**, 13 (1999).

³A. A. Istratov, T. Buonassisi, E. R. Weber, R. J. McDonald, A. R. Smith, R. Schindler, J. Isenberg, J. Kalejs, J. Rand, P. Geiger, G. Hahn, J. P. Rakotoniaina, and O. Breitenstein, *NCPV Rev. Meeting*, Denver, CO, 2003 (unpublished).

⁴D. Macdonald, A. Cuevas, A. Kinomura, and Y. Nakano, *J. Appl. Phys.* **97**, 033523 (2005).

⁵P. S. Plekhanov, R. Gafiteanu, U. M. Gosele, and T. Y. Tan, *J. Appl. Phys.* **86**, 2453 (1999).

⁶T. Buonassisi, A. A. Istratov, S. Peters, C. Ballif, J. Isenberg, S. Riepe, W. Warta, R. Schindler, G. Willeke, Z. Cai and B. Lai, *Appl. Phys. Lett.* **87**, 121918 (2005).

⁷T. Buonassisi, A. A. Istratov, M. A. Marcus, B. Lai, Z. Cai, S. M. Heald, and E. R. Weber, *Nat. Mater.* **4**, 676 (2005).

⁸W. B. Henley and D. A. Ramappa, *J. Appl. Phys.* **82**, 589 (1997).

⁹A. Haarahiltunen, H. Väinölä, O. Anttila, M. Yli-Koski, and J. Sinkkonen, *J. Appl. Phys.* **101**, 043507 (2007).

¹⁰P. Zhang, H. Väinölä, A. A. Istratov, and E. R. Weber, *Appl. Phys. Lett.* **83**, 4324 (2003).

¹¹R. A. Frosch and A. M. Salama, U.S. Patent No. 4,311,870 (9 January 1982).